Available online at www.sciencedirect.com

ScienceDirect

Journal of the European Ceramic Society 35 (2015) 2587–2592

www.elsevier.com/locate/jeurceramsoc

Flash sintering incubation in Al_2O_3/TZP composites

E. Bichaud [a,b,*], J.M. Chaix [b], C. Carry [b], M. Kleitz [a], M.C. Steil [a]

[a] *Laboratoire d'Electrochimie et de Physicochimie des Matériaux et des Interfaces (LEPMI) – UMR 5631 CNRS-Université de Grenoble Alpes, BP 75, 38402 Saint Martin d'Hères, France*

[b] *Laboratoire de Science et Ingénierie des Matériaux et Procédés (SIMaP) – UMR 5266 CNRS-Université de Grenoble Alpes, BP 46, 38402 Saint Martin d'Hères, France*

Received 23 January 2015; received in revised form 27 February 2015; accepted 28 February 2015
Available online 12 March 2015

Abstract

The flash sintering incubation process was characterized with Al_2O_3/TZP composites in isothermal furnace experiments. The compositions in tetragonal zirconia, TZP and Al_2O_3 were 0, 20, 40 and 60 vol.% of Al_2O_3. AC electrical field E_0 (1000 Hz) of 100 or 200 V/cm was used. The current density was limited at 10 or 20 A/cm^2, and the pre-heating temperatures were 900, 1000 and 1100 °C. The flash phenomenon depends on the overall conductivity of the sample. For a constant electrical field, the incubation time only depends on the sample overall conductivity whatever its temperature or composition. The power density supplied to the sample is the key parameter. The incubation time is affected by the heat losses, which mainly occur by thermal conduction through the electrode contacts, as evidenced by the marked influence of the sample geometry. A simple energy balance equation accounts for the observed current variations.

Keywords: Flash sintering; Al_2O_3/TZP composites; Incubation period; Electrical conductivity; Thermal runaway

1. Introduction

Flash sintering is an ECAS (electrical current activated sintering) technique which enables the densification of ceramic powder compacts in less than 5 s, at much lower furnace temperatures than conventional sintering.[1] Firstly evidenced with yttria-stabilized zirconia, the capability of this new sintering process has been reported for a broadening range of ceramic materials[2–7] and recently for composite materials.[8] Currently, it is raising a large interest in material processing science.

The flash sintering elementary mechanisms are not yet fully understood. It has been recognized that the sudden onset of sintering is accompanied by an abrupt increase in the material conductivity and of the resulting current density through the specimen. Most of the experiments reported in the literature are conducted under constant applied electric field. The Joule heating and the associated specimen temperature increase have been studied, modelled and compared to the temperatures required for an equivalent conventional densification.[9–11] Several physical and chemical phenomena have been suggested to be responsible for the flash triggering and flash densification. Cologna et al. first suggested that the local heating due to the particle–particle contact resistance would enhance diffusion.[1] The nucleation of Frenkel pairs has also been proposed.[1,2,12] Another proposed interpretation is a local sintering pressure[12] which could drive vacancies into the grain boundaries and interstitial ions into the pores, inducing densification while electron–hole pairs contribute to a higher electrical conductivity. A recent approach assumes that the interaction between the external field and the space charge layer along the grain surfaces could change the diffusion kinetics during the flash sintering.[12–14]

Flash sintering was initially evidenced and studied under constant furnace heating rate and constant applied electric field. In this case, flash sintering occurs in a few seconds at a furnace threshold temperature; the higher the electric field, the lower this threshold temperature. Flash sintering has later also been studied in isothermal furnace conditions.[9,10] The flash sintering onset is in this case observed after a lead time which depends

* Corresponding author at: Laboratoire d'Electrochimie et de Physicochimie des Matériaux et des Interfaces (LEPMI) – UMR 5631 CNRS-Université de Grenoble Alpes, BP 75, 38402 St. Martin d'Hères, France. Tel.: +33 476826652.
E-mail address: Emmanuelle.bichaud@lepmi.grenoble-inp.fr (E. Bichaud).

http://dx.doi.org/10.1016/j.jeurceramsoc.2015.02.033
0955-2219/

on the magnitude of the applied electric field and on the furnace temperature. In the literature, this time Δt is called incubation period.[8]

In this paper, we report experimental results on this lead time or incubation period, obtained with oxide-oxide particulate composites, by applying the electric field when the temperature is stabilized (isothermal furnace conditions). Ceramic–ceramic composites constituted by a conductive phase (ZrO_2–3%Y_2O_3) and an insulating one (Al_2O_3) with different volume fractions were used to investigate the effect of the sample conductivity on the flash incubation.

2. Experimental

2.1. Materials, sample processing and characterization

All the samples were prepared from pre-mixed alumina–zirconia composite powders provided by Baikowski, France. The blends were constituted by tetragonal zirconia, TZP (partially stabilized with 3 mol% Y_2O_3) and α-Al_2O_3. The alumina contents were: 0, 20, 40 and 60 vol.%. The samples were uniaxially pressed at 20 MPa, then isostatically cold pressed under a pressure (150–250 MPa) adapted in order to obtain a green relative density of 49 ± 1%. The cylindrical specimens were 8 mm in diameter (flat surfaces $S_1 \approx 0.5\,cm^2$) and about 5 mm high. Fig. 1 shows two micrographs of the compacted samples containing 20, and 60 vol.% alumina, before sintering. The SEM observations confirm the typical grain sizes deduced from BET data on single phase powders: 80 nm for zirconia and 100 nm for alumina. The two phases are homogeneously distributed.

2.2. Flash-sintering equipment and procedure

The experimental set-up was described in a previous paper,[10] electric field is applied to the sample through platinum electrodes (10 mm diameter and 0.5 mm thick discs) in contact with the ceramic. It enables the flash sintering of cylindrical samples connected on its flat surfaces, and enables to monitor the shrinkage during the experiment. To improve the uniformity of the current distribution through the samples, these surfaces were covered with Pt paint (Metalor® 6926). The current collectors made of Pt were slightly pressed against the surfaces. The experiments were performed in air. The samples were heated up to the preheating temperature T_0 at 10 °C/min. The sample temperature was stabilized at T_0 during 30 min before applying the electric field. All temperatures mentioned henceforth refer to T_0. A thermocouple was placed close to the sample (at about 1 mm), allowing a good measurement of T_0 before the application of the field, and an indication of the temperature increase when the flash occurs. The AC voltage was provided by a Pacific Smart Source 115ASX AC power generator, controlled by the UPC Manager V.1.4 software. The electrical parameter variations were continuously recorded. The current densities and electric fields reported in this paper were calculated using the recorded current intensity through the sample and the green body dimensions. The sample length contraction was continuously recorded.

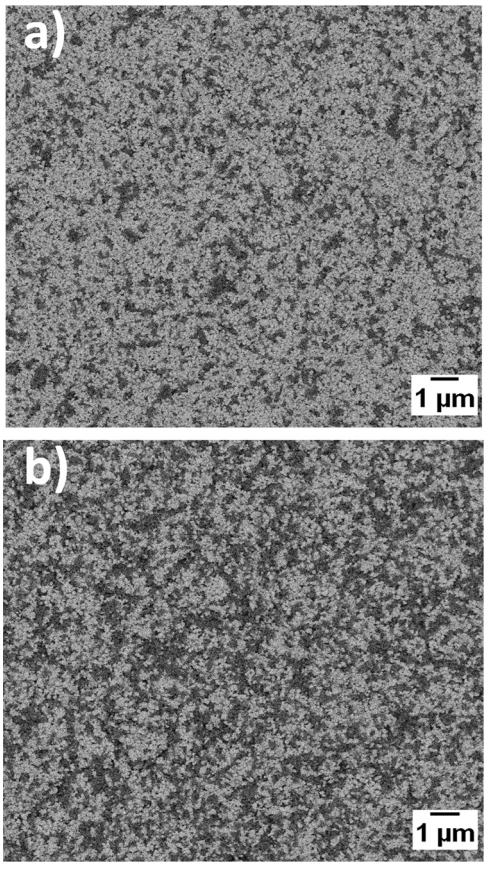

Fig. 1. SEM (BSE mode) view of the fracture of the alumina–zirconia compacts before sintering: with 20 (a) and 60 (b) vol.% alumina. The light grey phase is zirconia, the dark grey one is alumina, and pores are black.

As described in literature[15] the isothermal flash sintering process involves three main stages (Fig. 2) when the constant electrical field E_0 is applied:

- Stage I: "incubation". Under a constant electrical field (E_0), the current density I remains low, with a very slow evolution for a lead time Δt before the flash event. The measurement of this parameter needs an arbitrary definition: in this paper, we decided to define Δt as the time to reach a current density of 2 A/cm^2, which marks the sharp onset of the current increase: this value is low with respect to the current densities reached during the flash but, significantly larger than the initial current

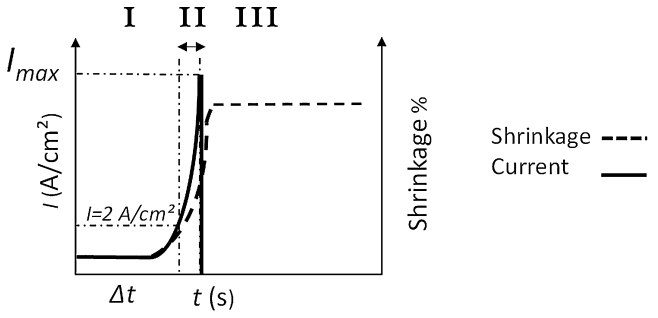

Fig. 2. Schematic view of an isothermal flash sintering experiment (the field is applied at $t = 0$): evolution of current density and shrinkage.

values, which always remain below 0.5 A/cm^2. In this paper, we have arbitrarily limited our observations to 300 s. Although longer delay times have been reported in the literature,[8] our study is focused on experimental conditions which lead to a flash before 300 s.

- Stage II: "flash current increase". After this incubation time, the current density I abruptly increases. The onset of the sample densification is synchronous with the sudden current density increase. Over this transient period, the large current upsurge results in a power spike, which would lead to a device breakdown and sample damage.
- Stage III: "current limited stage". When a predefined current density I_{max}, is reached, the power supply is therefore either switched from voltage control to current control, so that the current density is maintained constant during a predefined period, or switched down to zero. It is to be noticed that densification can continue during a short period, even after the field is cut off.

The aim of the paper is to characterize the dependence of the incubation time Δt on the sample conductivity and on other experimental parameters, accordingly, we disconnected the applied field at the end of the second stage. Four values of the pre-heating temperature T_0 were studied: 800, 900, 1000 and 1100 °C. Two values of the 1000 Hz AC field were studied: 100 V/cm and 200 V/cm. The maximum current density I_{max} at which the power supply was switched down was either 10 or 20 A/cm^2.

2.3. Sample electrical conductivity

The sample conductivities were measured by impedance spectroscopy at 400 °C and at all the temperatures T_0 of our experiments, before and after sintering, using a HP4194A impedancemeter in a frequency range of 100–1.5 × 10^7 Hz and with a 500 mV signal amplitude. Fig. 3 shows the impedance diagrams of the 0, 20 and 40 vol.% alumina samples, at 900 °C, before sintering. This method allows us to distinguish the sample resistance and the contact resistance between the sample and the electrodes. For all compositions, the sample resistance is deduced from the high frequency loop (>10^3 Hz, see Fig. 3). As expected, the sample overall resistance R_0 increases when the alumina content increases. The sample initial overall conductivity σ_0 of the composites at each composition is plotted versus temperature in Fig. 4, showing that the selected compositions and temperatures enable to cover a wide range of sample conductivities. To verify the influence of alumina on the electrical proprieties of our composites, we fabricated fully dense samples by conventional sintering (10 °C/min up to 1500 °C, without dwell). The conductivities of these samples were measured at different temperatures. They vary according to the usual relationship:

$$\sigma = \sigma_0 e^{-(Q/kT)} \quad (1)$$

with an activation energy Q of 0.85 eV, whatever the composite composition, in good agreement with the literature values for yttria doped zirconia.[16] (This activation energy was slightly modified by the contribution of contact resistances. This will not be discussed here).

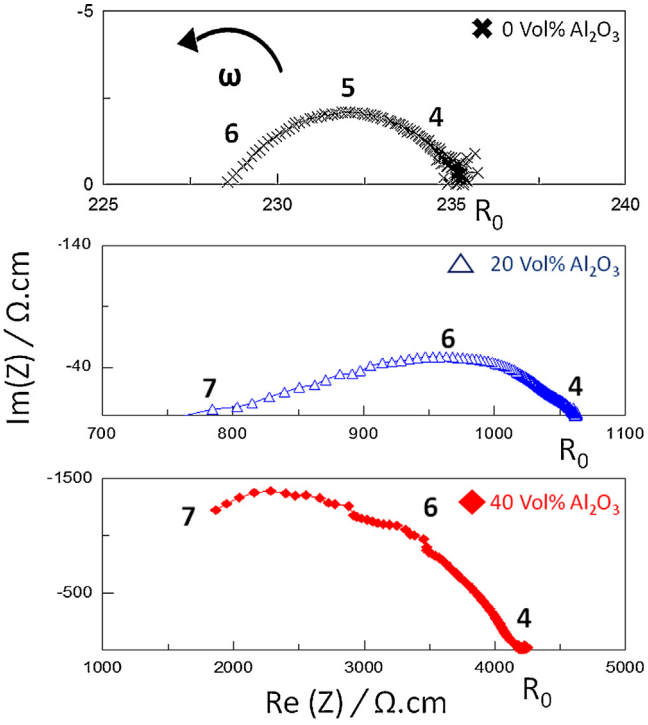

Fig. 3. Impedance diagrams of green body samples (0, 20 and 40 vol.% Al_2O_3) at 900 °C. The numbers n indicate signal frequency ($f = 10^n$ Hz).

3. Results and discussion

The experimental parameters and results are summarized in Table 1. It must be reminded that when no significant increase of the current was observed after 300 s, it was concluded that no flash phenomenon would occur. A flash with 35 s incubation time is observed at T_0 = 800 °C with pure TZP. For a pre-heating temperature of 900 °C, flash sintering is observed only with pure TZP (Fig. 5a) and not with 20 or 40 vol.% alumina. At 1100 °C, all samples with up to 40 vol.% alumina experience a flash sintering (Fig. 5b). Samples with 60 vol.% alumina, tested at 1100 °C and 200 V/m, showed no flash before 300 s.

Fig. 6 summarizes the observed behaviours for the two values of the applied electric field. It enables a rough estimation of the

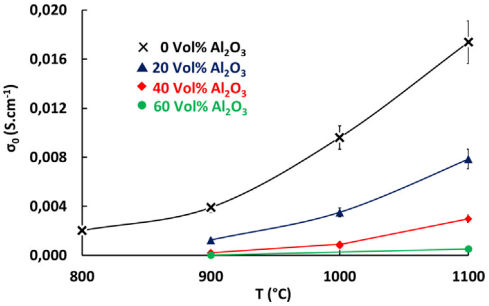

Fig. 4. Effective conductivity measured before the application of the electric field.

Table 1
Summary of experiments: conditions, measured conductivity before the field application and measured incubation time.

Al_2O_3 (vol.%)	T_0 (°C)	σ_0 (S/cm)	Δt (s) at $E_0 = 100$ V/m	Δt (s) at $E_0 = 200$ V/m
0	800	2.0E−03	35.6	∼0
	900	3.9E−03	8.9	∼0
	1000	9.6E−03	∼0	∼0
	1100	1.7E−02	∼0	∼0
20	900	9.1E−04	No flash	10.7
	1000	2.8E−03	26.2	2.61
	1100	8.7E−03	7.5	∼0
40	900	2.1E−04	No flash	No flash
	1000	8.6E−04	No flash	19.7
	1100	3.0E−03	56.8	6.2
60	1100	5.2E−04	(Not tested)	No flash

limits in the composition/temperature diagram, which separate flash domains from those with no flash for each value of the applied field. At given T_0 and E_0 values, the incubation time Δt significantly increases with the alumina content; compositions showing no flash can be viewed as experiments with an infinite incubation time.

Fig. 7 shows the incubation time as a function of the initial overall conductivity, for the samples flashed under 100 and 200 V/cm. These curves include all the points recorded at different temperatures T_0 and sample compositions. The first observation is that, under a given applied field E_0, all the

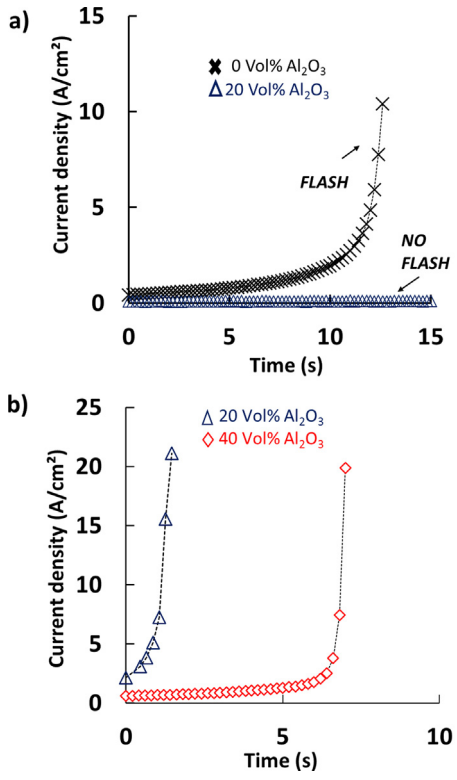

Fig. 5. Current density evolution in isothermal flash sintering of alumina-zirconia composites: (a) $T_0 = 900$ °C and $E_0 = 100$ V/cm (flash for zirconia, no flash for 20 vol.% alumina and above composites); (b) $T_0 = 1100$ °C and $E_0 = 200$ V/cm (incubation sensitivity to alumina content).

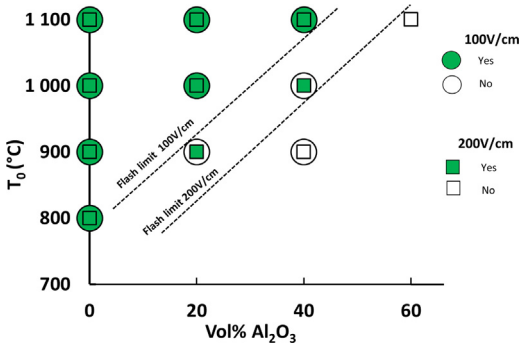

Fig. 6. Flash sintering occurrence in the composition/temperature domain for 100 V/cm (circles) and 200 V/cm (squares). Green symbols indicate flash sintering while empty symbols indicate that no flash is observed. (For interpretation of the references to colour in this figure legend, the reader is referred to the web version of this article.)

experimental points are on a single curve, whatever the initial temperature T_0 and sample composition. This clearly confirms that the sample conductivity is a determining parameter, at a given applied electric field.

A second observation is that each curve shows that the incubation time tends towards infinity for a non-zero conductivity value. It defines a threshold value $\sigma_{threshold}$ for the initial overall conductivity. When the initial sample conductivity σ_0 is lower than this limit, no flash phenomenon is observed. For an applied field of 100 V/cm, the threshold value is around 2×10^{-3} S/cm and for 200 V/cm, it is 8×10^{-4} S/cm. From an experimental point of view, the comparison of these two values and of the relative positions of the two curves in Fig. 7 indicates that the lower the sample conductivity, the higher the applied electric field required to initiating a flash. This is consistent with a reported flash sintering of zirconia obtained at 390 °C and 2250 V/cm, after quite a long time.[17] When the sample effective conductivity is much higher than $\sigma_{threshold}$, the incubation period vanishes and the flash proper starts immediately.

One of the sources of the flash phenomenon is the Joule heating. The Joule power dissipated inside the sample is proportional to $E_0^2\sigma$, where σ is the sample conductivity. In Fig. 8, the incubation time was plotted versus the initial value $E_0^2\sigma_0$. As in Fig. 7, all the experimental points which have lead to a flash event, whatever the experimental values of T_0, E_0 and composition, appear to lie on a single curve. This demonstrates that the initial

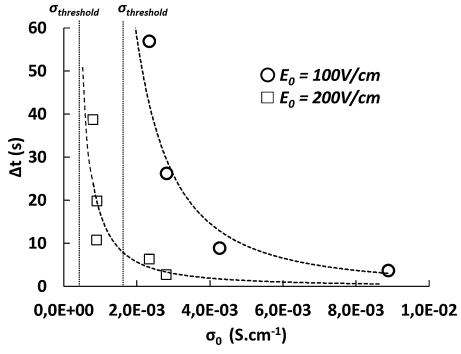

Fig. 7. Incubation time versus initial apparent sample conductivity for the set of experiments of Table 1 (all compositions and temperatures).

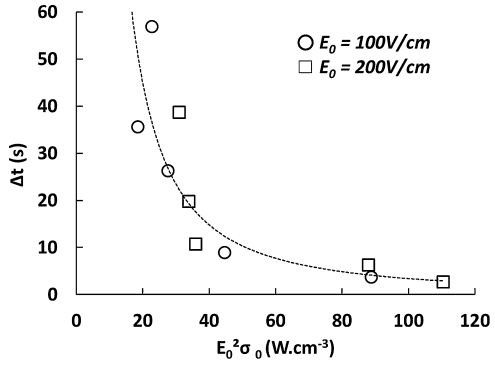

Fig. 8. Incubation time versus initial power density from all compositions for the experiments of Table 1 which lead to the flash phenomenon.

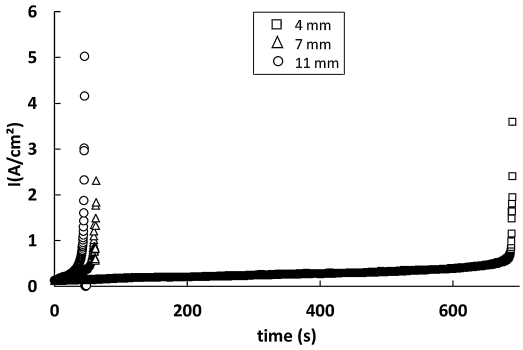

Fig. 9. Flash sintering incubation for different sample lengths (40 vol.% Al_2O_3, $T_0 = 1100\,^{\circ}C$, $E_0 = 130$ V/cm).

Joule power density supplied to the sample acts as a major parameter of the incubation time. The incubation time vanishes when the power density is high: in this case, the heat produced by Joule effect rapidly increases the temperature, which in turn drastically increases the conductivity, due to the strong nonlinear increase of the conductivity with temperature (Eq. (1)), leading to a classic thermal runaway.

Fig. 8 also shows that the incubation time increases to infinity for a nonzero threshold value of the initial energy density, in agreement with the results of Table 1 showing that no flash occurs when the initial conductivity is low at a given value of E_0. This suggests that, in order to produce the flash event, the Joule effect needs to overcome the thermal losses due to heat exchange with the surroundings (furnace). The dissipation of a part of the energy supplied to the sample can be due to a thermal conduction process through the electrode contacts and to the thermal radiation of the sample free surface.

The energy balance can be roughly written in as:

$$VC\frac{dT}{dt} = P_{Joule} - P_{losses} \tag{2}$$

where V and C are, respectively, the sample volume and heat capacity per unit volume.

When the heat losses are not negligible with respect to the Joule heat production, the temperature will need some time before reaching a value at which the thermal runaway starts, When the heat losses are relatively more important, the temperature will stop increasing before reaching the runaway value, this resulting in no flash.

The samples used in the experiments were cylinders of radius r and height h. The field was applied on the flat surfaces ($S_1 = \pi r^2$) and the side surface ($S_2 = 2\pi rh$) was in contact with the furnace atmosphere. The energy production is proportional to the sample volume ($V = \pi r^2 h$):

$$P_{Joule} = E_0^2 \sigma Sh = \pi E_0^2 \sigma r^2 h \tag{3}$$

While the heat losses occur through the surfaces S_1 and S_2:

$$P_{losses} = k_1 2S_1(T - T_0) + k_2 S_2(T - T_0) = k_1 2\pi r^2(T - T_0) + k_2 2\pi rh(T - T_0) \tag{4}$$

In which k_1 and k_2 are effective heat transfer coefficients at surfaces S_1 and S_2, respectively. Note that this first order approximation is only used here in the first stage of Joule heating (incubation regime), when T remains close to T_0 (it is clear that on surface S_2, this is a rough linear approximation of radiative transfer).

Combining Eqs. (2)–(4) leads to an indicator of the temperature increase rate during the incubation period:

$$C\frac{dT}{dt} = E_0^2\sigma - k_1\frac{2}{h}(T - T_0) - k_2 2\frac{1}{r}(T - T_0) \tag{5}$$

This equation indicates an effect of the sample characteristics r and h, i.e., of its shape and size, on the temperature increase rate. To evaluate the part played by the energy dissipation and evaluate on which surface the heat losses are predominant, additional experiments were performed.

This second series of experiments is based on cylindrical samples of the same radius r (cross-sectional area S_1) and different heights h: 4, 7 and 11 mm, respectively. They were made of the 40 vol.% alumina composite and pre-heated at 1100 °C. A constant field of 130 V/cm was applied. The results (Fig. 9) clearly show the sensitivity of the incubation time with the sample height: the higher the sample, the smaller the incubation time. This means that, at constant radius, the relative values of the energy loss decrease when h increases, showing that the term $k_1(2/h)(T - T_0)$ is predominant in the heat losses in our experiments. In other words, the heat losses are mainly driven by conduction through the electrode contacts. These results show that the flash incubation characteristics markedly depend on the sample geometry. Accordingly, it will be difficult to compare results obtained with dog-bone-shaped samples which are relatively thin and long, to those relevant to cylindrical samples. Moreover, in dog bone situations, heat losses are mainly by radiation across the sample free surface, and not through the electrodes, which are just point contacts.[11]

4. Conclusions

Experiments based on different Al_2O_3/TPZ composite compositions show the influence of the sample overall initial conductivity on the lead time before the flash event. For each value of the applied electrical field, a threshold value $\sigma_{threshold}$ of the sample conductivity is the experimentally relevant parameter which determines the flash occurrence. When the sample initial conductivity is lower than $\sigma_{threshold}$ the incubation time

tends to infinity and no flash phenomenon is observed, after a reasonable experimental time. It is demonstrated that the initial power density supplied to the sample and not the electrical field, is the determining electrical parameter for the onset of the flash phenomenon. This supplied power density (proportional to $E_0^2\sigma$) depends on the electrical field and on the material conductivity.

A regular heating process correctly accounts for the incubation parameter variations. This conclusion agrees with the latest publication by Todd et al.[18] which indicates that the flash event can be seen as a consequence of runaway Joule heating under voltage control caused by the rapid reduction of the sample resistivity with increasing temperature.

The energy dissipation from the sample is a key feature of the incubation process. It naturally explains why too low a power density supply cannot lead to a flash. In the case of cylindrical samples, as those investigated in this paper, the prevalent dissipation mechanism is the thermal conduction through the electrode contacts. Conversely, in the case of dog-bone shaped samples used in many other laboratories, a prevalent radiation process through the free sample surface has been reported.

Acknowledgements

The Baikowski Company is thanked for providing the powder blends.

References

1. Cologna M, Rashkova B, Raj R. Flash sintering of nanograin zirconia in <5 s at 850 °C. *J Am Ceram Soc* 2010;**93**(11):3556–9.
2. Cologna M, Francis JSC, Raj R. Field assisted and flash sintering of alumina and its relationship to conductivity and MgO-doping. *J Eur Ceram Soc* 2011;**31**(15):2827–37.
3. Prette ALG, Cologna M, Sglavo V, Raj R. Flash-sintering of Co_2MnO_4 spinel for solid oxide fuel cell applications. *J Power Sources* 2011;**196**(4):2061–5.
4. Muccillo R, Muccillo ENS. Electric field-assisted flash sintering of tin dioxide. *J Eur Ceram Soc* 2014;**34**(4):915–23.
5. Yoshida H, Sakka Y, Yamamoto T, Lebrun J-M, Raj R. Densification behaviour and microstructural development in undoped yttria prepared by flash-sintering. *J Eur Ceram Soc* 2014;**34**(4):991–1000.
6. Jha SK, Raj R. The effect of electric field on sintering and electrical conductivity of titania. *J Am Ceram Soc* 2013;**97**(2):527–34.
7. Zapata-Solvas E, Bonilla S, Wilshaw PR, Todd RI. Preliminary investigation of flash sintering of SiC. *J Eur Ceram Soc* 2013;**33**(13–14):2811–6.
8. Naik KS, Sglavo VM, Raj R. Flash sintering as a nucleation phenomenon and a model thereof. *J Eur Ceram Soc* 2014;**34**(15):4063–7.
9. Francis JSC, Raj R. Influence of the field and the current limit on flash sintering at isothermal furnace temperatures. *J Am Ceram Soc* 2013;**93**(9):2754–8.
10. Steil MC, Marinha D, Aman Y, Gomes JRC, Kleitz M. From conventional ac flash-sintering of YSZ to hyper-flash and double flash. *J Eur Ceram Soc* 2013;**33**(11):2093–101.
11. Raj R. Joule heating during flash-sintering. *J Eur Ceram Soc* 2012;**32**(10):2293–301.
12. Raj R, Cologna M, Francis JSC. Influence of externally imposed and internally generated electrical fields on grain growth, diffusional creep, sintering and related phenomena in ceramics. *J Am Ceram Soc* 2011;**94**(7):1941–65.
13. Conrad H, Yang D. Dependence of the sintering rate and related grain size of yttria-stabilized polycrystalline zirconia (3Y-TZP) on the strength of an applied DC electric field. *Mater Sci Eng A* 2011;**529**(29–30):8523–9.
14. Yang D, Conrad H. Enhanced sintering rate and finer grain size in yttria-stabilized zirconia (3Y-TZP) with combined DC electric field and increased heating rate. *Mater Sci Eng A* 2011;**528**(3):1221–5.
15. Naik KS, Sglavo VM, Raj R. Field assisted sintering of ceramic constituted by alumina and yttria stabilized zirconia. *J Eur Ceram Soc* 2014;**34**(10):2435–42.
16. Weller M. Oxygen mobility in yttria-doped zirconia studied by internal friction, electrical conductivity and tracer diffusion experiments. *Solid State Ionics* 2004;**175**(1–4):409–13.
17. Downs JA, Sglavo VM. Electric field assisted sintering of cubic zirconia at 390 °C. *J Am Ceram Soc* 2013;**96**(5):1342–4.
18. Todd RI, Zapata-Solvas E, Bonilla RS, Sneddon T, Wilshaw PR. Electrical characteristics of flash sintering: thermal runaway of Joule heating. *J Eur Ceram Soc* 2015;**35**(6):1865–77.